RSC Advances

PAPER

View Article Online
View Journal | View Issue

Cite this: *RSC Adv.*, 2020, **10**, 36125

Improving the solubility and bioavailability of anti-hepatitis B drug PEC *via* PEC–fumaric acid cocrystal†

Long Li, *[a] Xian-Hong Yin[b] and Kai-Sheng Diao[b]

Received 30th July 2020
Accepted 23rd September 2020

DOI: 10.1039/d0ra06608g

rsc.li/rsc-advances

PEC is a new generation of phosphamide ester anti-hepatitis B virus drug. It is a prodrug of tenofovir and can be rapidly metabolized to tenofovir. However, its poor solubility in water (0.219 mg mL^{-1} at 25 °C) has limited its oral bioavailability. In this study, we aimed to improve the solubility and consequently the oral bioavailability of PEC *via* a cocrystal. A cocrystal of PEC with fumaric acid (FUA) (PEC–FUA, 1 : 1) was successfully obtained and characterized. The crystal structure of this cocrystal was tested using a single crystal X-ray diffraction method. The intrinsic dissolution rate (IDR) characterization was performed in a pH 6.8 buffer. The solubility of this cocrystal in 0.1 M HCl (pH 1.0) and pH 6.8 phosphate buffers was investigated, and the results showed that the solubility of the cocrystal was 3.8 and 4.0 times that of free PEC, respectively. We also studied the pharmacokinetics of beagle dogs. The mean $AUC_{0-24\ h}$ of the cocrystal is about 4.2 times that of free PEC, indicating that the solubility and bioavailability of PEC can indeed be improved by forming the cocrystal. It may become an ideal solid form of an active pharmaceutical ingredient suitable for pharmaceutical preparations, and it can be further studied later.

Introduction

In recent years, the research on cocrystals has become increasingly fierce, especially in the pharmaceutical industry.[1–10] In the pharmaceutical field, a drug cocrystal is a crystalline solid containing at least one active pharmaceutical ingredient (API) and one or more cocrystal coformers (CCFs). These substances exist in one crystal lattice, and the molecules connected through non-ionic way interacting.[11] To the best of our knowledge, there are polymorphic, amorphous, salt-forming, and cocrystal methods for changing the properties, especially solubility, of pharmaceutical active ingredients.[12–18] The polymorphic form is very limited in improving the solubility of poorly soluble drugs. Although amorphous drugs can improve a certain solubility, their stability is generally problematic. Although salt formation can greatly improve the solubility of drugs, there are certain requirements for the degree of ionization. The cocrystal can improve the solubility of the drug,[19–33] the bioavailability[34,35] and the stability,[36–39] and there is no limit to the degree of ionization of the drug.

Tenofovir is a nucleotide DNA polymerase and reverse transcriptase inhibitor with anti-HBV and HIV activity, and its phosphamide ester derivatives have been approved by the FDA for the treatment of hepatitis B virus.[40] PEC (Scheme 1) is a new generation of phosphamide esters anti-hepatitis B virus drug. It is a prodrug of tenofovir and can be rapidly metabolized to tenofovir. Due to its low solubility in water (0.219 mg mL^{-1}), its bioavailability is limited. Therefore, it is very important to develop its new solid form formulation to improve solubility and ultimately to improve bioavailability. PEC contains ionizable group (–NH–), which can form salts, but the salt formation screening test found that solids cannot be obtained after salt formation. PEC contains amino and purine groups, which can form hydrogen bonding force[41–43] with CCFs, connect CCFs with it to form a cocrystal, and obtain a solid that can improve solubility.

PEC contains one amino and one purine group. PEC molecules are connected into a one-dimensional chain through the NH···O intermolecular hydrogen bonding force. PEC molecules can form hydrogen bonding force with carboxyl and hydroxyl groups, so a series of CCFs containing carboxyl and hydroxyl groups are used to link with PEC molecules (Table 1). And obtained a cocrystal of PEC molecule and fumaric acid (FUA).

The cocrystal was characterized by elemental analysis, Fourier transform infrared spectroscopy analysis, thermodynamics research, powder X-ray diffraction and single crystal X-ray diffraction techniques. The powder dissolution, intrinsic dissolution rate, pharmacokinetics and dynamic vapor sorption were also investigated.

[a]*Sichuan Kelun Pharmaceutical Research Institute Co., Ltd., Chengdu 610000, China. E-mail: llgxmd@163.com; Fax: +86-28-85417785*

[b]*College of Chemistry and Chemical Engineering, Guangxi University for Nationalities, Nanning, 530006, China*

† Electronic supplementary information (ESI) available: FTIR spectra. CCDC 2016017. For ESI and crystallographic data in CIF or other electronic format see DOI: 10.1039/d0ra06608g

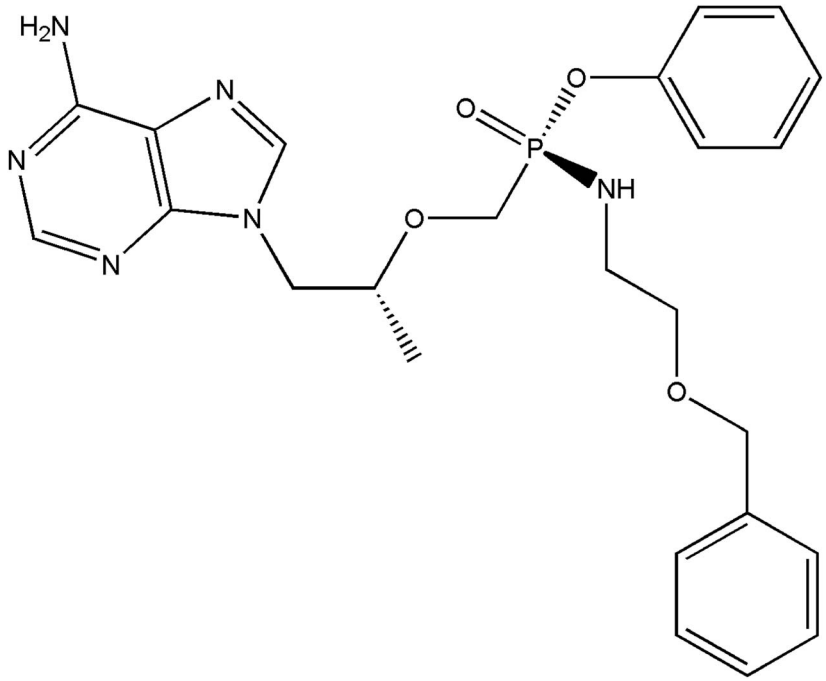

Scheme 1 Chemical structures of PEC.

Table 1 Coformer library used in cocrystal screening

S/N	Cofomer
1	Glycolic acid
2	Malic acid
3	Adipic acid
4	Fumaric acid
5	Benzoic acid
6	L-Tartaric acid

Experimental section

Materials and general methods

PEC (>99%) was provided by Sichuan Kelun Pharmaceutical Research Institute Co., Ltd. Fumaric acid (99%) were purchased from Chron Chemicals Corporation. Methanol and acetonitrile of high-performance liquid chromatography (HPLC) grade were purchased from Merck. All the other reagents were analytical grade and commercially available with out further purification. Elemental analyses were characterized by an Perkin Elmer 2400 II elemental analyzer. The infrared spectra were recorded in the 4000–400 cm^{-1} region using KBr pellets and a Perkin Elmer 100FT-IR. Thermogravimetric analyses (TGA) was recorded on a TGA (METTLER TOLEDO) instrument with a heating rate of 10 °C min^{-1}. Differential scanning calorimetry (DSC) was recorded on a DSC1 (METTLER TOLEDO) instrument with a heating rate of 10 °C min^{-1}. Powder X-ray diffraction (PXRD) patterns were obtained on a PANalytical XPert3 Powder Diffractometer with Cu Kα radiation (45 kV, 40 mA).

PEC–fumaric acid cocrystal (1 : 1)

PEC (496.5 mg, 100 mmol) and Fumaric acid (116 mg, 100 mmol) were dissolved in ethanol (10 mL) at 50 °C. The solution was cooled to room temperature. Then, 15 mL of acetonitrile

Table 2 Crystal data and structure refinement for PEC–FUA

Empirical formula	$C_{28}H_{33}N_6O_8P$
Formula weight	612.57
Temperature/K	293.15
Crystal system	Monoclinic
Space group	$P2_1$
a/Å	13.7013(6)
b/Å	6.4058(4)
c/Å	17.3373(10)
α/°	90
β/°	96.021(5)
γ/°	90
Volume/Å^3	1513.25(14)
Z	2
ρ_{calc} g cm^{-3}	1.344
μ/mm^{-1}	0.149
F(000)	644.0
Crystal size/mm^3	0.35 × 0.3 × 0.25
Radiation	Mo Kα (λ = 0.71073)
2Θ range for data collection/°	5.98 to 52.738
Index ranges	$-11 \le h \le 17$, $-5 \le k \le 8$, $-21 \le l \le 20$
Reflections collected	7082
Independent reflections	4629 [R_{int} = 0.0256, R_{sigma} = 0.0531]
Data/restraints/parameters	4629/1/401
Goodness-of-fit on F^2	1.024
Final R indexes [$I > 2\sigma(I)$]	R_1 = 0.0456, wR_2 = 0.0985
Final R indexes [all data]	R_1 = 0.0596, wR_2 = 0.1093
Largest diff. peak/hole/e Å^{-3}	0.26/−0.27
Flack parameter	0.06(9)

Table 3 Hydrogen bond distances and angles for PEC–FUA cocrystal

D–H···A	*d*(D–H)	*d*(H···A)	*d*(*D*···A)	∠DHA
N(5)–H(5B)···O(5)	0.860	2.048	2.901(3)	171.15(2)
N(5)–H(5A)···O(2)#1	0.861	2.080	2.934(2)	171.74(2)
O(6)–H(6C)···N(4)	0.931	1.734	2.647(2)	166.05(2)
O(8)–H(8)···N(2)#2	0.956	1.841	2.735(2)	154.58(2)

Symmetry codes: #1, $-x$, $-0.5 + y$, $2 - z$; #2, $1 + x$, y, z

was added over 5 minutes. A crystalline precipitate formed and stirred for 3 hours. The white product was filter and dried under vacuum at 45 °C overnight. Yield: 85% based on PEC. Put the filtrate in a glass bottle, seal with a parafilm, tile small holes, and evaporate slowly at room temperature. After 5 days, needle-shaped crystals of PEC–fumaric acid cocrystal were obtained. Anal. calcd for $C_{28}H_{33}N_6O_8P$: C, 54.85; H, 5.38; N, 13.71%. Found: C, 54.81; H, 5.32; N, 13.79%. IR data (KBr, cm^{-1}): 3320, 3237, 3147, 2907, 2867, 2599, 1901, 1717, 1694, 1671, 1614, 1579, 1494, 917, 761, 645.

Single-crystal X-ray diffraction

Single-crystal X-ray diffraction data for the PEC–fumaric acid cocrystal were collected on a Xcalibur Eos diffractometer system with graphite monochromated Mo Kα radiation ($\lambda = 0.71073$ Å). The crystal was kept at 293.15 K during data collection. Using Olex2,[44] the structure was solved with the Superflip[45–47] structure solution program using Charge Flipping and refined with the ShelXL[48] refinement package using Least Squares minimisation. All nonhydrogen atoms were refined anisotropically. Hydrogen atoms were set in calculated positions and refined by a riding mode, with a common thermal parameter. The

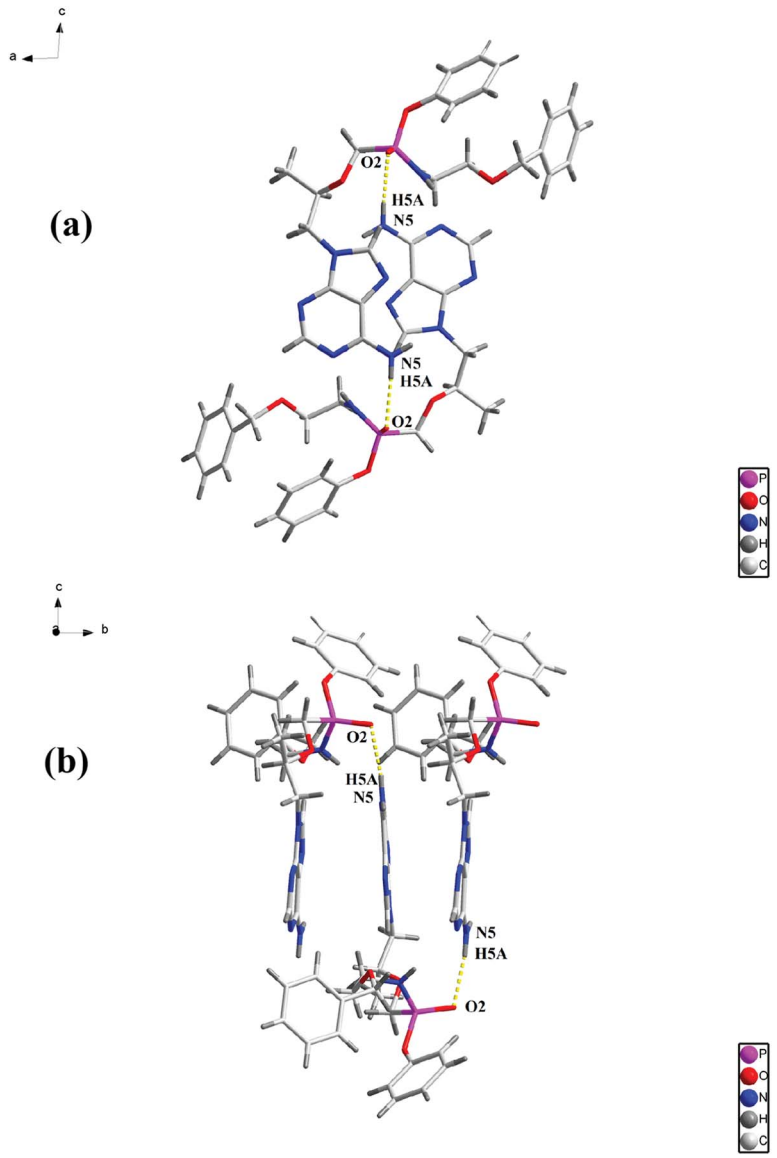

Fig. 1 View an 1D layer along (a) the *b* axis and (b) the *a* axis.

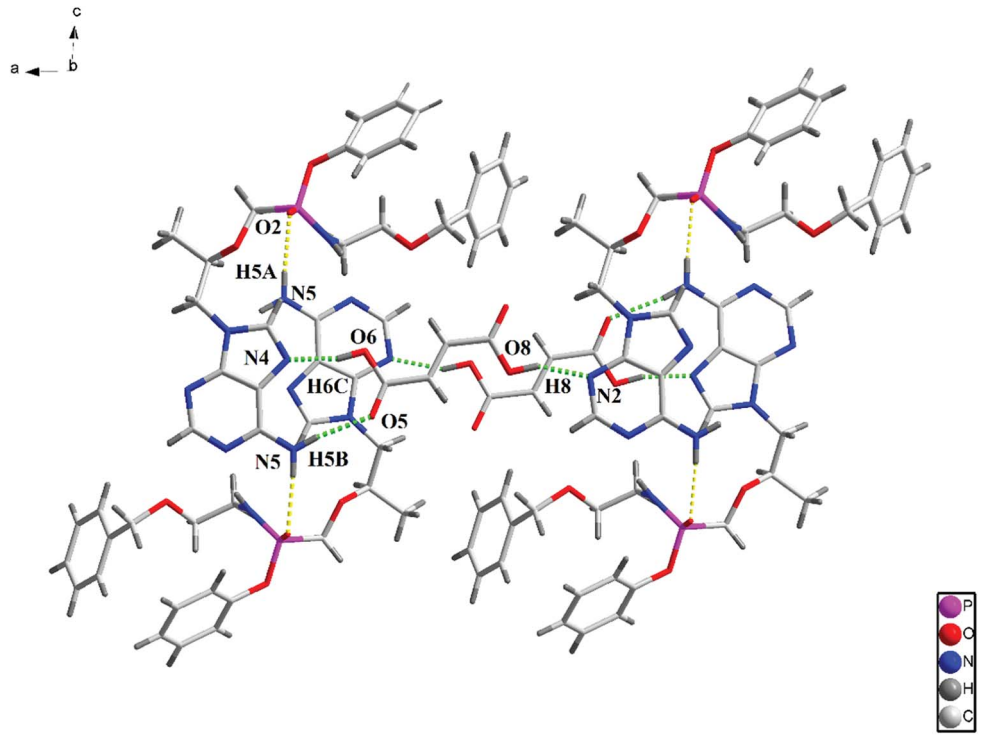

Fig. 2 View an 2D layer constructed by the hydrogen bonds along the *b* axis.

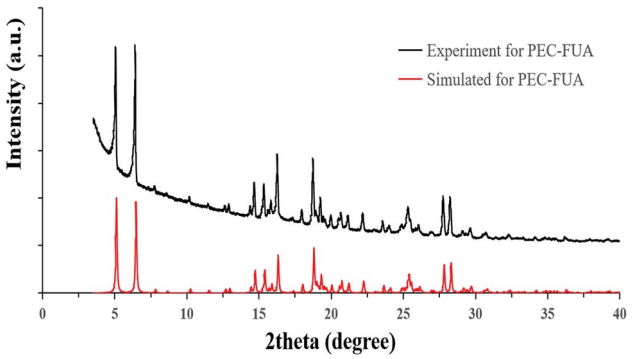

Fig. 3 Simulated and experimental PXRD patterns for PEC–FUA cocrystal.

crystallographic data and experimental details for the structure analysis are summarized in Table 2, and the hydrogen bonding distances and angles are given in Table 3.

Powder dissolution experiments

Grind PEC and PEC–fumaric acid cocrystal to obtain fine powder, sieving with multiple screens, and collect powder with a size in the range of 58–115 μm (use 250 mesh and 125 mesh screen) for powder solubility test. Throw 100 mg PEC powder and 100 mg PEC–FUA cocrystal powder into the solution of hydrochloric acid medium (50 mL, 0.1 M, pH 1.0) and phosphate buffered saline (PBS) (50 mL, 0.02 M, pH 6.8) to ensure that the solids can be excessive. Keep stirring at a speed of 100 rpm at 37 °C, take multiple samples at the specified time and test the solubility. Filter and dilute the obtained solution and place it in the high performance liquid chromatography (Aglient 1260) for detection with a wavelength of 254 nm. The analytical column was XBridge C18 (4.6 × 150 mm, 3.5 μm). Column temperature is 30 °C. Injection volume is 20 mL. Injection concentration is 0.2 mg mL^{-1}. Dipotassium hydrogenphosphate buffer solution (20 mM, pH 10.5) (eluent A) and acetonitrile (eluent B) at a flow rate of 1.0 mL min^{-1}. The gradient elution program starts with 20% B, keep for 3 minutes, increase to 40% in 13 minutes, increase to 80% in 3 minutes, keep for 3 minutes, and then returns to the 25% in 3 minutes and keep for 3 minutes.

Pharmacokinetics in beagle dogs plasma

The male beagle dogs used in the experiment were provided by the animal research center of Sichuan Kelun Pharmaceutical Research Institute Co., Ltd. All the animal experiments were carried out in accordance with institutional guidelines in compliance with regulations formulated by Sichuan Kelun Pharmaceutical Research Institute Co., Ltd. The experimental protocol was approved by the Institutional Animal Care and Use Committee of Sichuan Kelun Pharmaceutical Research Institute Co., Ltd. The pharmacokinetic experiment used 6 male beagle dogs, all weighting around 15 kg, free PEC and the PEC–fumaric acid cocrystal were administered orally to the beagle dogs at a specification of 1 mg kg^{-1}, open the mouth of the beagle dog, put the PEC and PEC co-crystal into the capsule, put it in the throat of the dog, and pour drinking water into the stomach with a syringe. After oral administration, blood samples were collected from the small saphenous vein on the lateral hindlimb

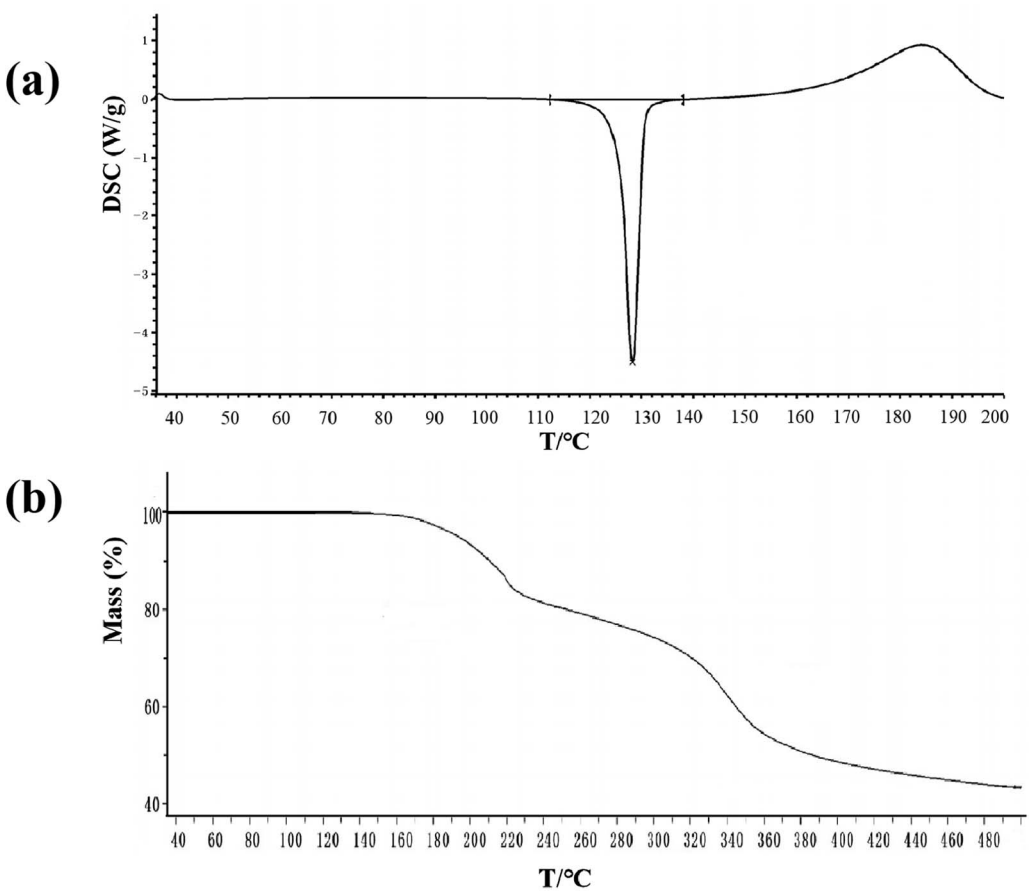

Fig. 4 DSC and TGA curves for PEC–FUA cocrystal.

of the beagle dog, with 2 mL blood taken each time, using a heparinized injector, at the following time intervals: 0.2, 0.5, 0.8, 1.1, 1.5, 3, 8, and 24 hours. Centrifuge the blood (10 min, 5000 rpm), and stored at −70 °C. 30 μL of plasma was mixed with 100 μL of acetonitrile containing 100 ng mL^{-1} of propranolol (used as the internal standard (IS)) and was vortexed for 10 min. After centrifugation (10 min, 5000 rpm), supernatant was mixed with Take the supernatant and mix it with methanol/water mixture (1 : 1) and inject it for LC-MS/MS analysis (Aglient 6120B).

Dynamic vapor sorption (DVS)

DVS study was performed on a DVS intrinsic instrument (Surface Measurement Systems, U.K.). The dried sample was placed in a nitrogen environment, and after equilibrium at 25 °C for 1 hour. The dynamic vapor sorption experiment was stared. The relative humidity is gradually increased from 0% to 90% with an interval of 10%, and the balance time is achieved by DM/DT mode. Then desorb from 90% to 0% in the same way.

Results and discussion

Crystal structure

The structure of the PEC–FUA cocrystal belongs to the monoclinic, $P2_1$ space group. The asymmetric unit contains one PEC and one FUA. After the formation of the cocrystal, PEC molecules are linked together through N5–H5A···O2 (2.080(3) Å) intermolecular hydrogen bonds to generate a one-dimensional (1D) chain (Fig. 1). The 1D chains are further connected by FUA through O6–H6C···N4 (1.734(3) Å), N5–H5B···O5 (2.048(3) Å) and O8–H8···N2 (1.841(3) Å) interlayer hydrogen bonds to form a 2D layer (Fig. 2).

PXRD and thermal analyses

PXRD was used to check the crystalline phase purity of the PEC–FUA cocrystal. The result shows that all the peaks displayed in the measured pattern of the PEC–FUA cocrystal closely match those in the simulated pattern generated from single-crystal diffraction data (Fig. 3), demonstrating the formation of pure crystalline phase of the PEC–FUA cocrystal. The DSC and TGA curves of the PEC–FUA cocrystal are shown in Fig. 4. From Fig. 4, it can be found that the cocrystal melts at 127 ± 2 °C (onset), fusion enthalpies is 86.75 J g^{-1} and then the cocrystal starts to decompose at the temperature of 140 ± 5 °C.

IR spectroscopy

The FTIR spectra for PEC–FUA cocrystal is show in Fig. S1 (ESI†), which exhibit two peaks at 1717 and 3320 cm^{-1}, which are assigned to the C=O stretching vibration and the O–H stretching absorption of the FUA, as well as N–H stretching

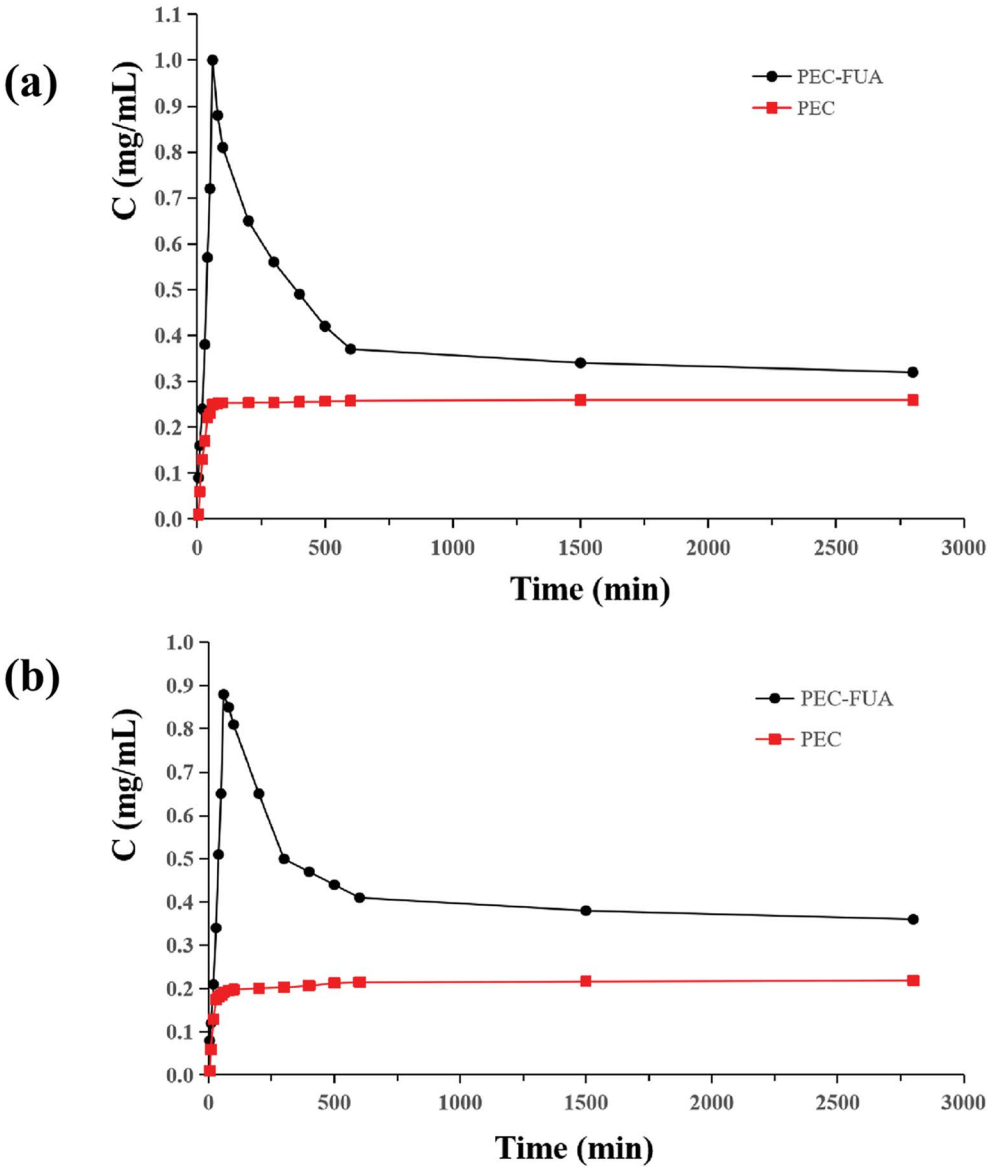

Fig. 5 Powder dissolution profiles for free PEC and PEC–FUA cocrystal in 0.1 M HCl (a), and 0.02 M phosphate buffer of pH 6.8 (b) at 37 °C within 48 h.

absorption peaks of the primary purine at 1579, 3147 and 3237 cm^{-1}, respectively, in which PEC–FUA cocrystal shows C=N stretching absorption peaks of the primary benzene ring at 1614 cm^{-1},and C–H stretching absorption peaks of the primary methyl at 2867 cm^{-1}. Shifts of C=O stretching frequency of the FUA and N–H stretching frequency of the primary purine comparing with that of the free PEC and FUA indicate the change of hydrogen bonding interactions on these functional groups in the PEC–FUA cocrystal.

Powder dissolution and IDR studies

The powder solubility of the drug substance has a great impact on the design of the formulation and the bioavailability of the drug. This is an important parameter that must be considered in drug development. The powder solubility curve of PEC and PEC–FUA cocrystal in pH 1.0 hydrochloric acid solution and pH 6.8 phosphate buffered saline buffer are shown in Fig. 5. It can be seen from the curve that the solubility and dissolution rate of PEC–FUA cocrystal are much larger than that of free PEC, and it can be seen that the solubility can indeed be improved after becoming a cocrystal. The maximum solubility of PEC–FUA cocrystal in pH 1.0 hydrochloric acid solution and pH 6.8 phosphate buffered saline buffer is 3.8 times and 4.0 times as large as those of free PEC. It can be found from the curve that PEC–FUA reaches the maximu solubility of free PEC. It can be found from the curve that PEC–FUA reaches the maximum solubility quickly, then slowly drops to a plateau, and is always higher than the solubility of free PEC. This solubility curve is very suitable for the pharmaceutical industry.[49–51] After the powder dissolution experiments, the undissolved solids were

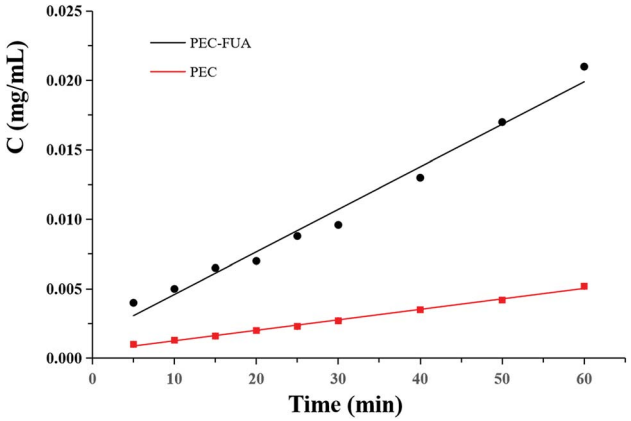

Fig. 6 IDR profiles for free PEC and PEC–FUA cocrystal in 0.02 M phosphate buffer of pH 6.8 at 37 °C.

Table 4 Mean pharmacokinetic parameters of free PEC and PEC–FUA cocrystal in male Beagle dogs

Parameter	PEC	PEC–FUA
$AUC_{0-24\ h}$ (h ng mL^{-1})	171	923
C_{max} (ng mL^{-1})	29.6	124
T_{max} (h)	1.12	1.25

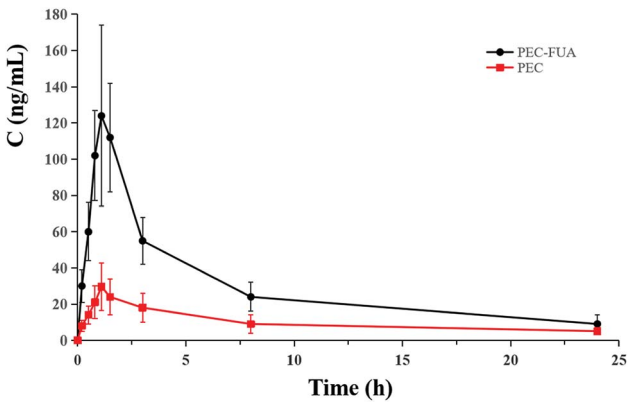

Fig. 7 Mean plasma concentrations *versus* time profiles of PEC following oral administration of free PEC (red square) and PEC–FUA cocrystal (black circle) in male beagle dogs. Each point represents the mean ± SD (n = 3).

filtered and dried under a vacuum, and the results of PXRD analysis indicated that part of the PEC–FUA cocrystal transformed to PEC form, while initial PEC maintains its crystal form after the dissolution experiments.

As far as we know, the intrinsic dissolution rate (IDR) of a drug has a great correlation with the absorption kinetics of the drug in the body. In order to obtain the data of the intrinsic dissolution rate of the drug, PEC–FUA and free PEC were tested in pH 6.8 phosphate buffered saline buffer. Several sampling tests were carried out within an hour. It can also be found from the curve (Fig. 6) that the linear correlation of PEC–FUA (R^2 =

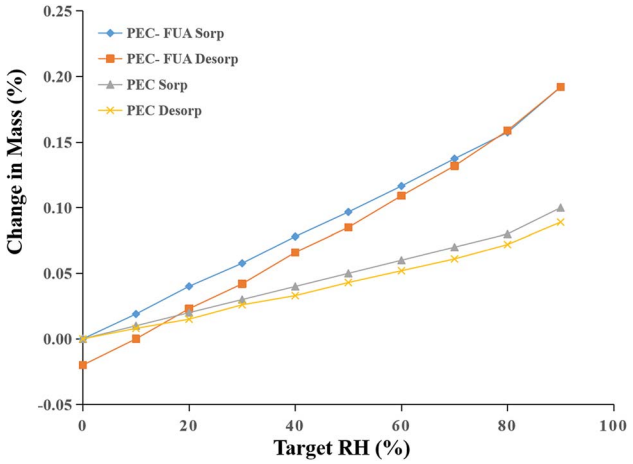

Fig. 8 DVS isotherm plots for free PEC and PEC–FUA cocrystal at 25 °C.

0.982) is not very good, which should be attributed to the shedding of fumaric acid in the medium. It can be seen from the curve that the intrinsic dissolution rate of PEC–FUA is much greater than that of PEC. The above experiment results show that PEC–FUA cocrystal can be used as a potential drug crystal for improving solubility and solubility rate in PEC formulations. After the IRD experiments, the undissolved solids were tested by PXRD analysis, which indicated that little PEC–FUA cocrystal transformed to PEC form due to a short time, and initial PEC also maintains its crystal form after the dissolution experiments.

Pharmacokinetics in beagle dogs plasma

Generally speaking, the increase in the powder solubility and intrinsic dissolution rate of the drug will help to improve the bioavailability of the drug *in vivo*. It can be seen from the experimental results of the powder solubility and intrinsic dissolution rate of PEC–FUA and PEC that the solubility and intrinsic dissolution rate of PEC drugs have been greatly improved after the formation of the cocrystal. In order to verify whether this increase is helpful for the increase in the bioavailability of PEC *in vivo*, we designed and conducted a beagle pharmacokinetic experiments. Experiments show that the beagle group taking PEC–FUA and the beagle group taking PEC have almost the same T_{max}, and the $AUC_{0-24\ h}$ and C_{max} of the beagle taking PEC–FUA are more than 3 times that of the beagle taking PEC (Table 4). From Mean plasma concentrations *versus* time profiles (Fig. 7), it can be known that between 0–8 h, the blood concentration of beagle dogs taking PEC–FUA is very high, which is very helpful for the treatment of diseases, and between 8–24 h, the blood drug concentration of beagle dogs taking PEC–FUA has decreased a lot, but it is still much higher than that of beagle dogs taking PEC. It can be seen from these experimental results that after PEC and fumaric acid become cocrystal, the powder solubility, intrinsic dissolution and bioavailability *in vivo* are greatly improved. These results have greatly encouraged the continued development of PEC drugs.

Dynamic vapor sorption (DVS)

Although PEC and FUA form a cocrystal, the solubility, IDR and bioavailability increase makes us very excited, yet will these increase greatly improve the hygroscopicity of API solids and affect its storage and preparation processes. Therefore, we conducted DVS tests on PEC–FUA and PEC to obtain their moisture absorption data. It can be seen from Fig. 8, that after forming the cocrystal, the moisture absorption of PEC–FUA in the humidity range of 0–90% is about 1 times higher than that of PEC. Although the hygroscopicity has been greatly improved, its actual value is still very low (<0.2%). In the pharmaceutical industry, this value indicates that it has no hygroscopicity. So, PEC and FUA still show non-hygroscopicity after forming a cocrystal. This property indicates that PEC–FUA cocrystal is very suitable for use as a pharmaceutical preparation.

Conclusions

For PEC, a poorly soluble drug, under the premise that the salt-type screening did not get a solid, we carried out a crystal engineering design on it, hoping to obtain a solid and improve its solubility and bioavailability. After passing the experiment, we successfully obtained the PEC–FUA cocrystal. For this cocrystal, we performed element analysis, infrared, thermal analysis, and PXRD detection. Its single crystal structure shows that there are many intermolecular hydrogen bonding forces in the cocrystal molecule, so that the cocrystal molecule can exist stably. Not only that, the powder solubility, IDR, and *in vivo* pharmacokinetic data of the cocrystal have been greatly improved compared with free PEC. Meanwhile, the hygroscopicity experiment after forming the cocrystal shows that it has almost no hygroscopicity, which is very beneficial for the storage of API and the production and preparation process of the formulation. In short, the acquisition of the PEC–FUA cocrystal is of great significance for the subsequent development of the drug PEC. Not only that, these findings also provide a good reference for the development of other innovative drugs.

Conflicts of interest

The authors declare no competing financial interest.

Acknowledgements

This work was supported by the Natural Science Foundation of China (No. 21567004).

References

1 B. Zhu, J. R. Wang, Q. Zhang, M. Q. Li, C. Y. Guo, G. B. Ren and X. F. Mei, Stable Cocrystals and Salts of the Antineoplastic Drug Apatinib with Improved Solubility in Aqueous Solution, *Cryst. Growth Des.*, 2018, **18**, 4701–4714.

2 D. X. Li, M. M. Kong, J. Li, Z. W. Deng and H. L. Zhang, Amine– carboxylate supramolecular synthon in pharmaceutical cocrystals, *CrystEngComm*, 2018, **20**, 5112–5118.

3 J. M. Li, X. L. Dai, G. J. Li, T. B. Lu and J. M. Chen, Constructing Anti-Glioma Drug Combination with Optimized Properties through Cocrystallization, *Cryst. Growth Des.*, 2018, **18**, 4270–4274.

4 G. Bolla and A. Nangia, Pharmaceutical cocrystals: walking the talk, *Chem. Commun.*, 2016, **52**, 8342–8360.

5 K. Suresh, V. S. Minkov, K. K. Namila, E. Derevyannikova, E. Losev, A. Nangia and E. V. Boldyreva, Novel Synthons in Sulfamethizole Cocrystals: Structure−property Relations and Solubility, *Cryst. Growth Des.*, 2015, **15**, 3498–3510.

6 K. Suresh, M. K. C. Mannava and A. Nangia, Cocrystals and Alloys of Nitazoxanide: Enhanced Pharmacokinetics, *Chem. Commun.*, 2016, **52**, 4223–4226.

7 S. P. Gopi, S. Ganguly and G. R. Desiraju, A Drug−Drug Salt Hydrate of Norfloxacin and Sulfathiazole: Enhancement of in Vitro Biological Properties via Improved Physicochemical Properties, *Mol. Pharmaceutics*, 2016, **13**, 3590–3594.

8 K. Suresh, N. R. Goud and A. A. Nangia, Solving Chemical Instability and Poor Solubility by Means of Cocrystals, *Chem.–Asian J.*, 2011, **8**, 3032–3041.

9 L. Fala, Entresto (Sacubitril/Valsartan); First-in-Class Angiotensin Receptor Neprilysin Inhibitor FDA Approved For Patients with Heart Failure, *Am. Health Drug Benefits*, 2015, **8**(6), 330–334.

10 D. Bernhardson, T. A. Brandt, C. A. Hulford, R. S. Lehner, B. R. Preston, K. Price, J. F. Sagal, M. J. St. Pierre, P. H. Thompson and B. Thuma, Development of an Early-Phase Bulk Enabling Route to sodium- Dependent Glucose Cotransporter 2 Inhibitor Ertugliflozin, *Org. Process Res. Dev.*, 2014, **18**, 57–65.

11 N. K. Duggirala, M. L. Perry, O. Almarsson and M. J. Zaworotko, Pharmaceutical cocrystals: along the path to improved medicines, *Chem. Commun.*, 2016, **52**, 640–655.

12 M. K. Bommaka, M. K. C. Mannava, K. Suresh, A. Gunnam and A. Nangia, Entacapone: Improving Aqueous Solubility, Diffusion Permeability, and Cocrystal Stability with Theophylline, *Cryst. Growth Des.*, 2018, **18**, 6061–6069.

13 L. S. Taylor and G. G. Z. Zhang, Physical chemistry of supersaturated solutions and implications for oral absorption, *Adv. Drug Delivery Rev.*, 2016, **101**, 122–142.

14 D. J. Berry and J. W. Steed, Pharmaceutical cocrystals, salts and multicomponent systems; intermolecular interactions and property based design, *Adv. Drug Delivery Rev.*, 2017, **117**, 3–24.

15 J. Bernstein, *Polymorphism in Molecular Crystals*, Oxford University Press, New York, NY, 2nd edn, 2019.

16 A. Bak, A. Gore, E. Yanez, M. Stanton, S. Tufekcic, R. Syed, A. Akrami, M. Rose, S. Surapaneni, T. Bostick, A. King, S. Neervannan, D. Ostovic and A. Koparkar, The Co-Crystal Approach to Improve the Exposure of a Water-Insoluble Compound: AMG 517Sorbic Acid Co-Crystal Characterization and Pharmacokinetics, *Journal of Pharmaceutical Sciences*, 2008, **97**(9), 3942–3956.

17 N. Shan, M. L. Perry, D. R. Weyna and M. J. Zaworotko, Impact of pharmaceutical cocrystals: the effects on drug pharmacokinetics, *Expert Opin. Drug Metab. Toxicol.*, 2014, **10**(9), 1255–1271.

18 N. Schultheiss and A. Newman, Pharmaceutical Cocrystals and Their Physicochemical Properties, *Cryst. Growth Des.*, 2009, **9**(6), 2950–2967.

19 L. D. Hughes, D. S. Palmer, F. Nigsch and J. B. O. Mitchell, Why Are Some Properties More Difficult To Predict than Others? A Study of QSPR Models of Solubility, Melting Point, and Log P, *J. Chem. Inf. Model.*, 2008, **48**, 220–232.

20 S. S. Kumar, R. Thakuria and A. Nangia, Pharmaceutical cocrystals and a nitrate salt of voriconazole, *CrystEngComm*, 2014, **16**(22), 4722–4731.

21 A. Y. Li, L. L. Xu, J. M. Chen and T. B. Lu, Phenazopyridine Cocrystal and Salts That Exhibit Enhanced Solubility and Stability | Crystal Growth & Design, *Cryst. Growth Des.*, 2015, **15**, 3785–3791.

22 J. Yao, J. M. Chen, Y. B. Xu and T. B. Lu, Enhancing the Solubility of 6-Mercaptopurine by Formation of Ionic Cocrystal with Zinc Trifluoromethanesulfonate: Single-Crystal-to-Single-Crystal Transformation, *Cryst. Growth Des.*, 2014, **14**, 5019–5025.

23 H. Y. He, Q. Zhang, J. R. Wang and X. F. Mei, Structure, physicochemical properties and pharmacokinetics of resveratrol and piperine cocrystals, *CrystEngComm*, 2017, **19**, 6154–6163.

24 K. Syrjanen, B. van Veen, J. Kiesvaara, H. A. Santos and J. Yliruusi, A new cocrystal and salts of itraconazole: Comparison of solid-state properties, stability and dissolution behavior, *Int. J. Pharm.*, 2012, **436**(1), 403–409.

25 Y. Yan, J. M. Chen, N. Geng and T. B. Lu, Improving the Solubility of Agomelatine via Cocrystals, *Cryst. Growth Des.*, 2012, **12**, 2226–2233.

26 D. J. Good and N. Rodríguez-Hornedo, Solubility Advantage of Pharmaceutical Cocrystals, *Cryst. Growth Des.*, 2009, **9**, 2252–2264.

27 K. Shiraki, N. Takata, R. Takano, Y. Hayashi and K. Terada, Dissolution Improvement and the Mechanism of the Improvement from Cocrystallization of Poorly Water-soluble Compounds, *Pharm. Res.*, 2008, **25**, 2581–2592.

28 C. B. Aakeroy, S. Forbes and J. Desper, Using Cocrystals To Systematically Modulate Aqueous Solubility and Melting Behavior of an Anticancer Drug, *J. Am. Chem. Soc.*, 2009, **131**, 17048–17049.

29 J. X. Song, J. M. Chen and T. B. Lu, Lenalidomide–Gallic Acid Cocrystals with Constant High Solubility, *Cryst. Growth Des.*, 2015, **15**, 4869–4875.

30 N. Rodríguez-Hornedo, S. J. Nehm, K. F. Seefeldt, Y. PaganTorres and C. J. Falkiewicz, Reaction Crystallization of Pharmaceutical Molecular Complexes, *Mol. Pharmaceutics*, 2006, **3**(3), 362–367.

31 J. R. Wang, C. J. Ye, B. Q. Zhu, C. Zhou and X. F. Mei, Pharmaceutical cocrystals of the anti-tuberculosis drug pyrazinamide with dicarboxylic and tricarboxylic acids, *CrystEngComm*, 2015, **17**, 747–752.

32 K. J. Paluch, L. Tajber, C. J. Elcoate, O. I. Corrigan, S. E. Lawrence and A. M. Healy, Solid-state characterization of novel active pharmaceutical ingredients: Cocrystal of a salbutamol hemiadipate salt with adipic acid (2:1:1) and salbutamol hemisuccinate salt, *J. Pharm. Sci.*, 2011, **100**, 3268–3283.

33 S. Cherukuvada, N. J. Babu and A. Nangia, Nitrofurantoin–p-aminobenzoic acid cocrystal: Hydration stability and dissolution rate studies, *J. Pharm. Sci.*, 2011, **100**, 3233–3244.

34 M. L. Cheney, N. Shan, E. R. Healey, M. Hanna, L. Wojtas, M. J. Zaworotko, V. Sava, S. Song and J. R. Sanchez-Ramos, Effects of Crystal Form on Solubility and Pharmacokinetics: A Crystal Engineering Case Study of Lamotrigine, *Cryst. Growth Des.*, 2010, **10**, 394–405.

35 A. I. Kitaigorodsky, *Mixed Crystals*, Springer Science & Business Media, Berlin, 2012.

36 R. Z. Lin, P. J. Sun, Q. Tao, J. Yao, J. M. Chen and T. B. Lu, Mechanism study on stability enhancement of adefovir dipivoxil by cocrystallization: Degradation kinetics and structure-stability correlation, *Eur. J. Pharm. Sci.*, 2016, **85**, 141–148.

37 J. R. Wang, C. Zhou, X. P. Yu and X. F. Mei, Stabilizing vitamin D_3 by conformationally selective co-crystallization, *Chem. Commun.*, 2014, **50**, 855–858.

38 A. V. Trask, W. D. S. Motherwell and W. Jones, Physical stability enhancement of theophylline via cocrystallization, *Int. J. Pharm.*, 2006, **320**, 114–123.

39 A. V. Trask, W. D. S. Motherwell and W. Jones, Pharmaceutical Cocrystallization: Engineering a Remedy for Caffeine Hydration, *Cryst. Growth Des.*, 2005, **5**, 1013–1021.

40 H. Chapman, M. Kernan, J. Rohloff, M. Sparacino and T. Terhorst, Purification of PMPA Amidate Prodrugs by SMB Chromatography and X-Ray Crystallography of the Diastereomerically Pure GS-7340, *Nucleosides, Nucleotides Nucleic Acids*, 2001, **20**, 1085–1090.

41 G. R. Desiraju, Supramolecular Synthons in Crystal Engineering—A New Organic Synthesis, *Angew. Chem., Int. Ed. Engl.*, 1995, **34**, 2311–2327.

42 G. R. Desiraju and T. Steiner, *The Weak Hydrogen Bond in Structural Chemistry and Biology*, IUCr Monographs in Crystallography, 1999.

43 S. Cherukuvada, N. J. Babu and A. Nangia, Nitrofurantoin−paminobenzoic acid cocrystal: Hydration stability and dissolution rate studies, *J. Pharm. Sci.*, 2011, **100**, 3233–3244.

44 O. V. Dolomanov, L. J. Bourhis, R. J. Gildea, J. A. K. Howard and H. Puschmann, OLEX2: a complete structure solution, refinement and analysis program, *J. Appl. Crystallogr.*, 2009, **42**, 339–341.

45 L. Palatinus and G. Chapuis, SUPERFLIP - a computer program for the solution of crystal structures by charge flipping in arbitrary dimensions, *J. Appl. Crystallogr.*, 2007, **40**, 786–790.

46 L. Palatinus and A. van der Lee, Symmetry determination following structure solution in P1, *J. Appl. Crystallogr.*, 2008, **41**, 975–984.

47 L. Palatinus, S. J. Prathapa and S. van Smaalen, EDMA: a computer program for topological analysis of discrete electron densities, *J. Appl. Crystallogr.*, 2012, **45**, 575–580.
48 G. M. Sheldrick, Crystal structure refinement with SHELXL, *Acta Crystallogr., Sect. C: Struct. Chem.*, 2015, **71**, 3–8.
49 M. K. Stanton and A. Bak, Physicochemical Properties of Pharmaceutical Co-Crystals: A Case Study of Ten AMG 517 Co-Crystals, *Cryst. Growth Des.*, 2008, **8**, 3856–3862.
50 M. K. Stanton, S. Tufekcic, C. Morgan and A. Bak, Drug Substance and Former Structure Property Relationships in 15 Diverse Pharmaceutical Co-Crystals, *Cryst. Growth Des.*, 2009, **9**, 1344–1352.
51 M. L. Cheney, D. R. Weyna, N. Shan, M. Hanna, L. Wojtas and M. J. Zaworotko, Supramolecular Architectures of Meloxicam Carboxylic Acid Cocrystals, a Crystal Engineering Case Study, *Cryst. Growth Des.*, 2010, **10**, 4401–4413.

